Original Article

All-trans retinoic acid (ATRA) inhibits insufficient radiofrequency ablation (IRFA)-induced enrichment of tumor-initiating cells in hepatocellular carcinoma

Song Wang[1*], Jingtao Liu[2*], Hao Wu[1], Anna Jiang[1], Kun Zhao[1], Kun Yan[1], Wei Wu[1], Haibo Han[3], Yanhua Zhang[2], Wei Yang[1]

Key Laboratory of Carcinogenesis and Translational Research (Ministry of Education/Beijing), [1]Department of Ultrasound; [2]Department of Pharmacy; [3]Department of Clinical Laboratory, Peking University Cancer Hospital & Institute, Beijing 100142, China

*These authors contributed equally to this work.

Correspondence to: Wei Yang. Key Laboratory of Carcinogenesis and Translational Research (Ministry of Education/Beijing), Department of Ultrasound, Peking University Cancer Hospital & Institute, No. 52 Fucheng Road, Haidian District, Beijing 100142, China. Email: 13681408183@163.com; Haibo Han. Key Laboratory of Carcinogenesis and Translational Research (Ministry of Education/Beijing), Department of Clinical Laboratory, Peking University Cancer Hospital & Institute, No. 52 Fucheng Road, Haidian District, Beijing 100142, China. Email: haibohan@bjmu.edu.cn; Yanhua Zhang. Key Laboratory of Carcinogenesis and Translational Research (Ministry of Education/Beijing), Department of Pharmacy, Peking University Cancer Hospital & Institute, No. 52 Fucheng Road, Haidian District, Beijing 100142, China. Email: zyh8812@163.com.

Abstract

Objective: Local recurrence of hepatocellular carcinoma (HCC) after radiofrequency ablation (RFA) treatment remains a serious problem. Tumor-initiating cells (TICs) are thought to be responsible for tumor relapse. Here, we investigated the effect of the TIC differentiation inducer, all-trans retinoic acid (ATRA), on RFA and explored the potential molecular mechanisms.

Methods: The proportions of $CD133^+$ and epithelial cell adhesion molecule $(EpCAM)^+$ TICs in recurrent HCC after RFA and primary HCC were first determined in clinic. Then, the effect of heat intervention or insufficient RFA (IRFA) on the malignant potential of HCC cells, including cell migration, sphere formation ability, tumor growth, the proportion of $CD133^+$ and $EpCAM^+$ TICs and expression of stem cell-related genes, was evaluated *in vitro* and *in vivo*. Finally, the effect of ATRA on the tumor growth and the proportion of TICs was evaluated.

Results: In clinical data, a higher proportion of $CD133^+$ and $EpCAM^+$ TICs was found in recurrent tumors than in primary tumors. *In vitro* heat intervention promoted the cell migration and sphere formation ability. Additionally, it increased the proportion of $CD133^+$ and $EpCAM^+$ TICs and the expression of stem cell-related genes. In addition, after IRFA the residual tumors in xenografts grew faster and had more TICs than untreated tumors. ATRA remarkably inhibited residual tumor growth after IRFA by elimination of TICs though the PI3K/AKT pathway. Combination treatment with ATRA resulted in longer survival outcomes in mouse xenografts than RFA alone.

Conclusions: ATRA, as a TIC differentiation inducer, could help to improve the effect of RFA treatment, which was partially attributed to its effect against TICs. The data indicated its potential as an alternative drug in the development of better therapeutic strategies for use in combination with RFA.

Keywords: Radiofrequency ablation; hepatocellular carcinoma; tumor-initiating cell; all-trans retinoic acid; tumor differentiation

Submitted Aug 11, 2021. Accepted for publication Oct 28, 2021.
doi: 10.21147/j.issn.1000-9604.2021.06.06
View this article at: https://doi.org/10.21147/j.issn.1000-9604.2021.06.06

Introduction

Hepatocellular carcinoma (HCC) is currently the 4th leading cause of cancer death worldwide (1), but the 2nd leading cause of cancer death in China accounting for nearly half deaths worldwide (2). Radiofrequency ablation (RFA) is considered one of the main potentially curative options, and it is minimally invasive, and easily performed in the treatment of early-stage HCC (3,4). However, the 5-year cumulative local recurrence rate after RFA has been reported to be 8%−15%, which makes it inferior to surgery as a local treatment (5). Prevention of post-RFA recurrence is clinically meaningful.

Tumor-initiating cells (TICs) are a small subpopulation of cancerous cells with self-renewal ability and long-term tumorigenic capacity responsible for tumor relapse (6). Previous studies have verified that the existence of TICs in human liver cancers is closely related to the malignant features of HCC, such as invasion, drug resistance, recurrence, metastasis, and poor prognosis (7,8). More importantly, some studies have proven that insufficient radiofrequency ablation (IRFA) could accelerate HCC recurrence related to the enrichment of TICs (9-11). Therefore, targeting TICs might be an effective strategy to prevent tumor recurrence after RFA therapy for HCC patients.

All-trans retinoic acid (ATRA) is a natural compound and the most potent therapeutic agent in acute myeloid leukemia because of its anti-proliferative, pro-apoptotic and pro-differentiating properties (12). Recent studies have shown that ATRA also has an antitumor role in solid cancers. ATRA can reduce cell cycle, promote apoptosis, and suppress gastric TIC properties in gastric cancer cells and patient-derived xenograft models (13,14). In pancreatic cancer, retinoic acid regulates the self-renewal capacity of cells by inducing partial differentiation of pancreatic tumor cells (15,16). In HCC, ATRA also shows dramatic efficiency in suppressing metastasis by combined chemotherapy with doxorubicin (17). ATRA remarkably reduces the proliferation, migration and invasion of the heap1−6 HCC cell line and effectively induces its differentiation through the reversal of epithelial-mesenchymal transition (EMT) (18). More importantly, ATRA can remarkably enhance the effect of cisplatin, which is at least partially due to ATRA-induced differentiation of HCC-TICs, and the subsequent decrease in chemoresistant subpopulation (19). Taken together, it seems that HCC is more sensitive to ATRA than other cancers, suggesting the prospective usefulness of ATRA in the treatment of HCC. However, the effects of ATRA on inducing differentiation of TICs after percutaneous RFA for HCC are not well clarified.

Here, this study reported that a dramatic enrichment of TICs in the recurrent HCC tumors after RFA resulted in rapid progression. This study also investigated the potential underlying mechanism and effects of ATRA on the enrichment of TICs after RFA treatment to prove the prospective usefulness of ATRA.

Materials and methods

Clinical specimens

A single-center retrospective analysis, consisting of 120 HCC patients who received ultrasound-guided percutaneous RFA therapy in Peking University Cancer Hospital from February 2004 to August 2006, was conducted. After RFA therapy, all patients underwent regular follow-up with contrast-enhanced computed tomography (CECT) or enhanced magnetic resonance imaging (MRI) and laboratory examinations. Ultrasound-guided core biopsy was performed in patients with primary HCC (n=75) and recurrent HCC (n=9) for pathological diagnosis. After matching, paired tumor samples were obtained in seven patients with both primary tumors before RFA and recurrent tumors after RFA. Tumor samples were collected with written informed consent and then fixed in paraffin blocks.

Cell culture

Human HCC cell lines, including HepG2, Huh7 and SK-Hep-1, were cultured in Roswell Park Memorial Institute (RPMI) 1640 medium, supplemented with 10% fetal bovine serum (FBS), 100 U/mL penicillin, and 100 μg/mL streptomycin (Invitrogen, Grand Island, NY, USA), in a humidified incubator containing 5% CO_2 at 37 °C.

Heat intervention

HepG2 and Huh7 cells were seeded into 6-well plates at 5×10^4 cells/well. After 24 h, the plates sealed within parafilm were submerged into a water bath at 42 °C for 6 h for maximum induction of heat shock protein 70 (HSP70) as described in our previous study (20). After heat intervention the cells were subsequently cultured for 48 h to remove debris and dead cells and used for the following experiments.

Sphere formation assay

One hundred single cells were plated in Ultra Low Attachment 96-well plates (Corning Incorporated Life Sciences, Acton, MA, USA) and cultured in Dulbecco's modified Eagle medium (DMEM)/F12 (Invitrogen) supplemented concluding with B27 (Invitrogen), 20 ng/mL epidermal growth factor, 10 ng/mL hepatocyte growth factor (PeproTech, Rocky Hill, NJ, USA), 20 ng/mL basic fibroblast growth factor (PeproTech), and 1% methylcellulose (Sigma) in a 5% CO_2 incubator for 3 weeks. Spheres larger than 100 μm were counted under a stereomicroscope (Olympus, Tokyo, Japan).

Wound healing assay

HepG2 cells were seeded in 6-well plates. Sterile pipette tips (200 μL) were used to scratch a straight line when cells grew to 80%−90% of a plate, and after washing three times with phosphate-buffer saline (PBS), the culture medium was replaced with serum free DMEM. An inverted microscope (Olympus) was used to observe the closure of the scratches in different groups at time points (0 and 24 h after the scratching).

Subcutaneous xenograft assay for HCC cells

Animal experiments were approved by the Institutional Animal Care and Use Committee of Peking University Oncology School. HepG2 and SK-Hep-1 cells (2×10^6 cells per mouse) were suspended in 200 μL serum-free DMEM and Matrigel (1:1) and then injected subcutaneously into the upper middle flank region of male NOD/SCID mice (5 weeks old). Tumor growth was monitored by periodic caliper measurement every 2−3 d by calculating the tumor volume according to the formula tumor volume = (longest diameter × shortest diameter^2)/2. The survival endpoint was a maximum tumor volume of 800 mm^3 or a survival of 4 weeks, whichever was reached first.

Animal model for recurrence HCC after IRFA treatment

For the recurrence model after IRFA, mice received percutaneous RFA under anesthesia induced via the intraperitoneal injection of pentobarbital sodium (45 mg/kg, Foshan, China) when the subcutaneous xenograft tumor volume reached 500−600 mm^3. Standard monopolar RFA was applied by using a 480-kHz RFA generator (Model CC-1-220; Valleylab, Tyco Health care, USA). Initially, the 0.7 cm tip of a 17-gauge electrically insulated electrode (ACT1507 electrode; Valleylab, Tyco Health care, USA) was placed into the tumor at half of the tumor along the longest diameter. RFA was applied for 5 min with the generator output titrated to maintain a designated tip temperature (65±2 °C). When the residual tumor grew 4 weeks after IRFA treatment, tumors were harvested from mice and sliced into 5 μm thick sections for pathological evaluation.

ATRA treatment in vivo

ATRA was prepared in dimethyl sulfoxide (DMSO) and administered slowly via intraperitoneal injection at concentrations of 10 mg/kg, 20 mg/kg and 40 mg/kg before 24 h of pre-RFA treatment for the first time. Subsequently, the drug was injected five times every two days.

Second tumorigenicity assay in vivo

For the second tumorigenicity assay, the xenograft tumor tissue was harvested at the end of the second week after different treatments (ATRA+IRFA, ATRA alone, and control). Fresh tumor tissues were mechanically minced and digested by collagenase IV, followed by primary culture in RPMI 1640 medium containing 10% fetal bovine serum after removal of fibroblasts. A total of 2×10^6 tumor cells per mouse were suspended in 200 μL serum-free DMEM and Matrigel (1:1) and then injected subcutaneously into the left and right flank regions of each NOD/SCID mouse (5 weeks old). Then, the second tumor growth was monitored every 2−3 d for 4 weeks. Tumorigenicity was recorded at the end of follow-up.

Immunohistochemistry staining

Tumor specimens were fixed in 4% formaldehyde overnight, embedded, and sliced into 5-μm thick sections. Tissues were stained with hematoxylin & eosin (H&E) for gross histopathologic analysis, with Ki-67 (Cell Signaling Technology, Danvers, USA) for cell proliferation and with CD34 (Abcam, San Francisco, USA) for vascular endothelial cells. Staining results were viewed under a light microscope, and five random high-powered fields were analyzed for each slide.

Immunofluorescence staining

Immunofluorescence staining was performed as described in previously protocol (21). Briefly, tumor tissues were snap

frozen in liquid nitrogen, embedded in optimal cutting temperature (OCT) compound, and sliced into 5-μm thick sections. CD31, HSP70, CD133 (APC-labeled, No. 130-090-854; Miltenyi Biotec), epithelial cell adhesion molecule (EpCAM) (FITC-labeled, No. 60136FI; Stemcell Technologies), Ki-67 and terminal deoxynucleotidyl transferase (TdT) dUTP nick-end labeling (TUNEL) staining results were viewed under an LSM 780 confocal microscope (Carl Zeiss, Jena, Germany).

Flow cytometric analysis (FCA)

For FCA, cells were dissociated with 0.02% ethylenediaminetetraacetic acid disodium salt, and HepG2 cells were resuspended in phosphate-buffered saline with 2% bovine serum albumin. Then, the cells were stained for 30 min at 4 °C with control or experimental antibodies. The surface makers CD133 (Miltenyi Biotec, Bergisch Gladbach, Germany) and EpCAM (EpCAM, BD Biosciences, San Jose, CA) were conjugated with fluorescein isothiocyanate (FITC), and the corresponding isotype immunoglobulin was used as a control. Fresh tumor tissues were digested and then single cells from xenografts were analyzed by FCA on a flow cytometer (Becton Dickinson, San Jose, CA, USA).

Quantitative real-time polymerase chain reaction (qRT-PCR)

TRIzol Reagent (Invitrogen, Carlsbad, CA, USA) was used to extract total RNA from HepG2 tumors. Two micrograms of RNA were reverse-transcribed into cDNA by Moloney murine leukemia virus reverse transcriptase (Invitrogen). qRT-PCR analysis was performed on an ABI7500 PCR machine using SYBR Green PCR Master Mix (Toyobo Co. Ltd., Osaka, Japan) and specific primers for each gene (*Table 1*). GAPDH was used as an endogenous reference and the expression differences were calculated by the $2^{-\Delta\Delta Ct}$ method.

Western blotting

Cells or homogenized tumor tissues were lysed in buffer (50 mmol/L Tris pH=7.4, 150 mmol/L NaCl, 1% NP-40, 0.25% sodium deoxycholate, 0.1% SDS) supplemented with 1 mmol/L phenylmethanesulfonyl fluoride (PMSF), phosphatase inhibitor cocktail, and protease inhibitor cocktail (Roche, Mannheim, Germany). Proteins were separated by 10% SDS-PAGE, transferred to PVDF membranes (75 V 1 h) and incubated with primary antibodies. The corresponding secondary HRP-conjugated goat anti-mouse or anti-rabbit antibodies were obtained from Jackson ImmunoResearch Laboratories Inc. (West Grove, PA). Immunocomplexes were detected with Western Chemiluminescent HRP substrate (Millipore, Billerica, USA). Photos were viewed with Image Acquisition using ImageQuant LAS 4000 (GE Healthcare, Pittsburgh, USA).

Statistical analysis

SPSS software (Version 21.0; IBM Corp., New York, USA) was used for statistical analysis. All continuous data are provided as the $\overline{x}\pm s$. Comparisons were performed by using one-way analysis of variance (one-way ANOVA) for multiple groups or unpaired student's *t*-test for two groups. Nemenyi test was used for paired comparisons and P values were adjusted accordingly. Categorical data were analyzed using Chi-square tests or Fisher's exact tests. Overall survival rates were calculated by the Kaplan-Meier method,

Table 1 Primer sequences used for qRT-PCR

Gene name	Sense	Anti-sense
Sox2	5'-ACATGAACGGCTGGAGCAAC-3'	5'-AGGAAGAGGTAACCACAGGG-3'
Oct-4	5'-GACAACAATGAAAATCTTCAGGAGA-3'	5'-CTGGCGCCGGTTACAGAACCA-3'
Nanog	5'-TGCCTCACACGGAGACTGTC-3'	5'-TGCTATTCTTCGGCCAGTTG-3'
α2δ1	5'-ACAGCAAGTGGAGTCAATCA-3'	5'-ACTGCTGCGTGCTGATAAGA -3'
KLF4	5'-AAGCCAAAGAGGGGAAGAC-3'	5'-CATCTGAGCGGGCGAATTTC-3'
MDR-1	5'-GCCTGGCAGCTGGAAGACAAATAC-3'	5'-ATGGCCAAAATCACAAGGGTTAGC-3'
ABCG2	5'-GGAGGCCTTGGGATACTTTGAA-3'	5'-GAGCTATAGAGGCCTGGGGATTAC-3'
BMI	5'-AGCAGCAATGACTGTGATGC -3'	5'-CAGTCTCAGGTATCAACCAG -3'
GAPDH	5'-GACCCCTTCATTGACCTCAAC-3'	5'-CTTCTCCATGGTGGTGAAGA-3'

qRT-PCR, quantitative real-time polymerase chain reaction.

and differences were analyzed with log-rank tests. Two-tailed P<0.05 was considered to indicate a statistically significant difference.

Results

CD133⁺ and EpCAM⁺ TICs were enriched in recurrent HCC tissues after IRFA treatment

Previously, it was reported that IRFA promoted HCC progression through the enrichment of CD133$^+$ TICs (22). A total of 120 patients with HCC (mean age: 61 years old; male percentage: 77%) who received ultrasound-guided percutaneous RFA in Peking University Cancer Hospital from 2004 to 2006 were enrolled in this part of the study. We observed the pathological findings of clinical tumor specimens by H&E staining. The results of H&E staining showed that the density of tumor cells was more intense in the recurrent tumor than in the primary tumor (*Figure 1Aa,b*). Meanwhile, on the CT imaging, the primary lesion presented as a round and well-defined tumor (*Figure 1Ac*, white arrow). However, the recurrent HCC after RFA was characterized as an irregular and poorly defined liver lesion near the area of necrosis (*Figure*

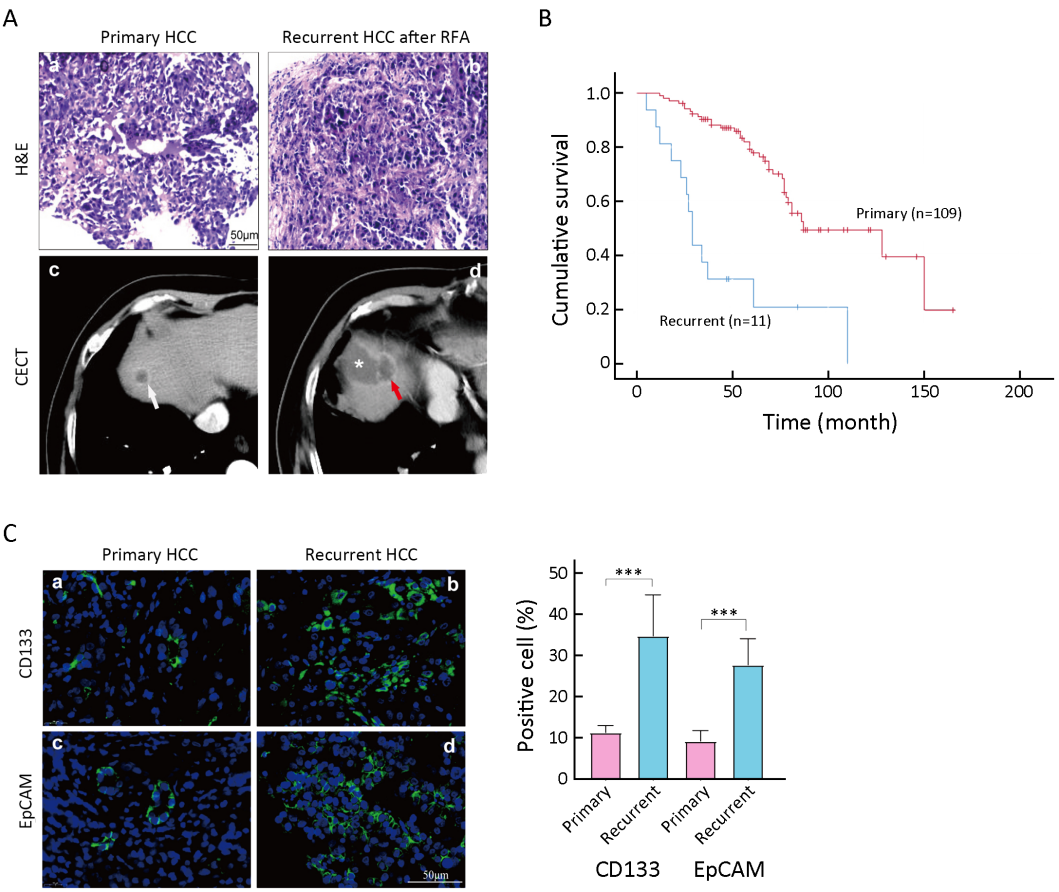

Figure 1 Enrichment of TICs in recurrent tissues after IRFA treatment. (A) Representative H&E staining (a,b) and CECT images of primary HCC (white arrow in c) and recurrent HCC (red arrow in d), * in d indicating the necrotic lesion of RFA treatment; (B) Overall survival rate for primary and recurrent HCC patients after RFA was compared using Kaplan-Meier analysis (P<0.05); (C) Immunofluorescence staining was used for detecting the expression of CD133⁺ and EpCAM⁺ TICs in primary and recurrent HCC tumors. Samples were obtained in seven patients with both primary tumors and recurrent tumors. Positive cells were stained with green signal; nuclei were stained with DAPI (blue). The bar graph in the right indicates the proportion of Ki-67⁺ and CD34⁺ cells as $\bar{x}\pm s$. TIC, tumor-initiating cell; IRFA, insufficient radiofrequency ablation; H&E, hematoxylin & eosin; CECT, contrast-enhanced computed tomography; HCC, hepatocellular carcinoma; RFA, radiofrequency ablation; EpCAM, epithelial cell adhesion molecule; DAPI, 4',6-diamidino-2-phenylindole. ***, P<0.001.

1Ad) after RFA treatment.

On the other hand, with a follow-up period of 160 (mean: 60.6±28.6) months, 11 (9.2%) patients were diagnosed with local recurrence, while others (109 patients, 90.8%) did not have recurrence. Among the 11 patients, 9 patients with recurrent tumors were treated by RFA again, and 2 were treated with transarterial chemoembolization (TACE). Consistent with our previous reports, patients with recurrent HCC had a significantly poorer overall survival time than patients without recurrence (48.9±11.6 months *vs*. 87.2±6.4 months, P<0.05, *Figure 1B*).

More importantly, both CD133$^+$ and EpCAM$^+$ TICs were significantly increased in recurrent HCC tissues (*Figure 1Cb*,*d*) compared with primary HCC tissues (*Figure 1Ca*,*c*). The enrichment of CD133$^+$ and EpCAM$^+$ TICs in recurrent tissues suggested that IRFA treatment might promote the stemness of tumor cells.

In vitro heat treatment enriches TICs in HCC cells

To mimic the effect of RFA on tumorigenic and invasive abilities *in vitro*, heat intervention was performed in HepG2 and Huh7 cells. Usually, the HSP70 protein can reflect the cell response to heat treatment (20). Thus, to determine the optimal heat treatment time for cancer cells, the level of HSP70 was analyzed by Western blot (42 and 45 °C) and immunofluorescence staining (*Figure 2A*,*B*). Subsequently, 42 °C for 6 h of heat intervention was used in the following cell experiments. Supporting our hypothesis, after heat treatment, the surviving cells displayed more rapid wound closure after 24 h compared with that in the control group (*Figure 2C*, 90.3%±3.1% *vs*. 60.7%±4.5%, P<0.001). As shown in *Figure 2D*, surviving cells after heat intervention displayed significantly higher sphere-forming ability than the control group (HepG2: 41.7%±4.1% *vs*. 8.7%±2.1%, P<0.001; Huh7: 36.5%±4.5% *vs*. 8.8%±3.3%, P<0.01). Additionally, FCA results suggested that CD133$^+$ and EpCAM$^+$ TICs increased from 3.0% to 36.0%, and 0.5% to 20.7%, respectively, in surviving cells after heat treatment (*Figure 2E*). Moreover, stem cell-related proteins, including SOX2, OCT4, MDR1, BMI and ABCG2, were all increased in the surviving cells after heat treatment (*Figure 2F*). The above results suggested that *in vitro* heat intervention could enrich TICs in HCC cells.

IRFA enriches TICs in vivo

As indicated in *Figure 3A*, we designed recurrent HCC after IRFA in a mouse xenograft model. As we expected, recurrent tumors after IRFA grew faster than those in the control group. Moreover, at the survival endpoint of the animal experiment, the tumor volume in the recurrent tumors after IRFA treatment was larger than that in the control group (732.7±204.6 mm^3 *vs*. 526.7±112.4 mm^3, P<0.05) (*Figure 3B*). The recurrent tumors included more proliferative cells stained with the nuclear proliferation biomarker Ki-67$^+$ and more CD34$^+$ cells representing for vascular endothelial cells (P<0.01 and P<0.001) (*Figure 3C*). Moreover, the recurrent tumors after IRFA treatment contained a higher proportion of CD31$^+$ (vascular index 0.44±0.03 *vs.* 0.17±0.06, P<0.01), CD133$^+$ (32.3%±5.8% *vs*. 20.2%±3.6%, P<0.05) and EpCAM$^+$ (22.4%±5.7% *vs*. 15.1%±4.4%, P<0.05) TICs than the control group (*Figure 3D*), indicating the enrichment of TICs after IRFA treatment. Consistently, the number of CD133$^+$ and EpCAM$^+$ TICs was also significantly increased by FCA (*Figure 3E*).

We performed a second IRFA treatment when the residual tumor grew to 10 mm in the longest diameter after the first IRFA and submitted to FCA for recurrent tumors after the 2nd IRFA treatment. As shown in *Figure 3F*, the percentages of CD133$^+$ cells and EpCAM$^+$ cells were further increased in the recurrent tumors treated with the second IRFA compared with those treated with the first IRFA (*Figure 3F*, CD133$^+$: 41.7%±3.6% *vs*. 28.9%±2.1%, P<0.05; EpCAM$^+$ 27.5%±4.3% *vs.* 18.7%±6.4%, P<0.05). In addition, there was a significant enrichment of CD133$^+$ cells at the fringe of the post-RFA necrosis region after 48 h of RFA treatment (*Figure 3G*). Compared with the control tumors, the recurrent tumors consistently expressed higher levels of genes associated with liver progenitor cells, including *EpCAM*, *OCT4*, *SOX2*, *NANOG*, *BMI*, *KLF4*, and *CTNNB*, by qRT-PCR (*Figure 3H*). Western blot analysis was further confirmed their increased expression at the protein level, including ABCG2, BMI, MDR1, OCT4, and SOX2 (*Figure 3I*). Taken together, these data suggested that the TICs exhibited heat resistance property and could be enriched in recurrent HCC tumors due to IRFA.

Collectively, the above results suggested that the recurrent tumors after IRFA treatment grew faster and contained more TICs.

ATRA suppresses growth of recurrent HCC after IRFA by inhibiting TICs

ATRA is currently used as a potential chemotherapeutic agent because of its antiproliferative, antioxidant and proapoptotic properties. In HCC, ATRA can reverse EMT

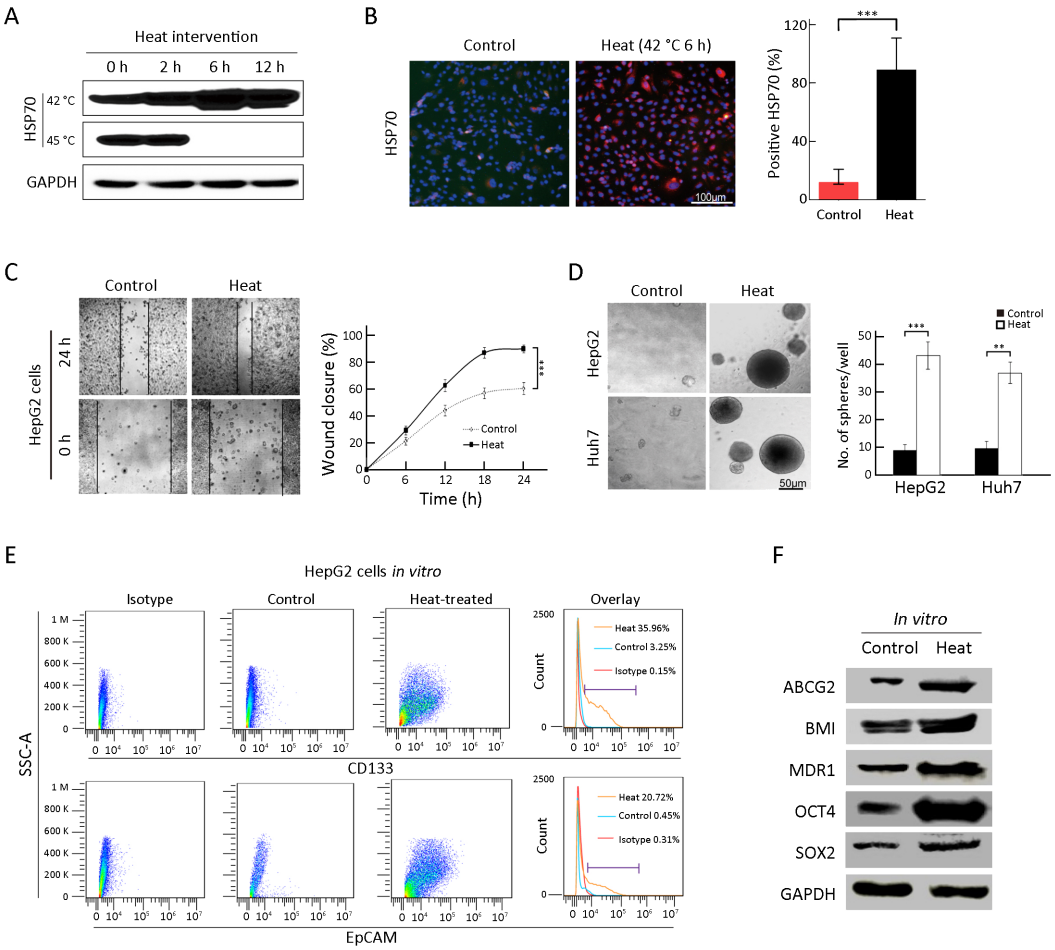

Figure 2 Enrichment of TICs by heat intervention *in vitro*. (A,B) Western blot (A) and immunofluorescence analysis (B) of HSP70 expression by heat treatment of HepG2 cells. Nuclei were stained with DAPI; (C) Wound healing analysis for the closure ability of HepG2 cells after heat treatment; (D) Sphere-forming ability of HepG2 and Huh7 cells after heat treatment. The number of spheres more than 50 μm was quantified; (E) Proportions of CD133$^+$ and EpCAM$^+$ subpopulation of HepG2 cells in the indicated treatment groups were analyzed by FCA; (F) Western blot analysis for the stem cell-related genes expression of HepG2 cells in control and heat treatment group. Bar graphs in (B,D) are presented as $\bar{x}\pm s$. TIC, tumor-initiating cell; HSP, heat shock protein; DAPI, 4',6-diamidino-2-phenylindole; EpCAM, epithelial cell adhesion molecule; FCA, flow cytometric analysis; SSC-A, side scatter area. **, P<0.01; ***, P<0.001.

in the antitumor process and potentiate the chemotherapeutic effect by inducing the differentiation of TICs in liver cancer (18,19). To investigate whether ATRA could suppress recurrent HCC after IRFA treatment by eliminating TICs, combination therapy was used. The sphere forming rate was dramatically decreased in the ATRA+heat group compared with the heat alone group *in vitro* (*Figure 4A*, HepG2: 23.4%±2.5% *vs*. 44.7%±3.1%, P<0.05; Huh7: 23.1%±3.5% *vs*. 36.5%±4.5%, P<0.05). In addition, the recurrent tumor growth and tumor weight in the ATRA treatment group after IRFA therapy were remarkably inhibited compared with IRFA alone in a dose-dependent manner for HepG2 tumors (P<0.05) (*Figure 4B*,*C*). Kaplan-Meier survival curves for mice also indicated that combination treatment could prolong survival time compared with IRFA alone (P<0.01) (*Figure 4D*). Consistently, compared with IRFA alone group, 20 mg/kg ATRA treatment in SK-Hep-1 cells also clearly suppressed the recurrent tumor growth and weight (P<0.01) (*Figure 4E*,*F*) and significantly prolonged the survival time of the mice (P<0.01) (*Figure 4G*). Moreover, the expression of TIC markers, including CD133 and EpCAM, was significantly reduced in the ATRA combinatorial treatment group, compared with the IRFA alone group, as shown by immunofluorescence staining (*Figure 4H*). Likewise, FCA suggested that the proportions of CD133$^+$ cells and

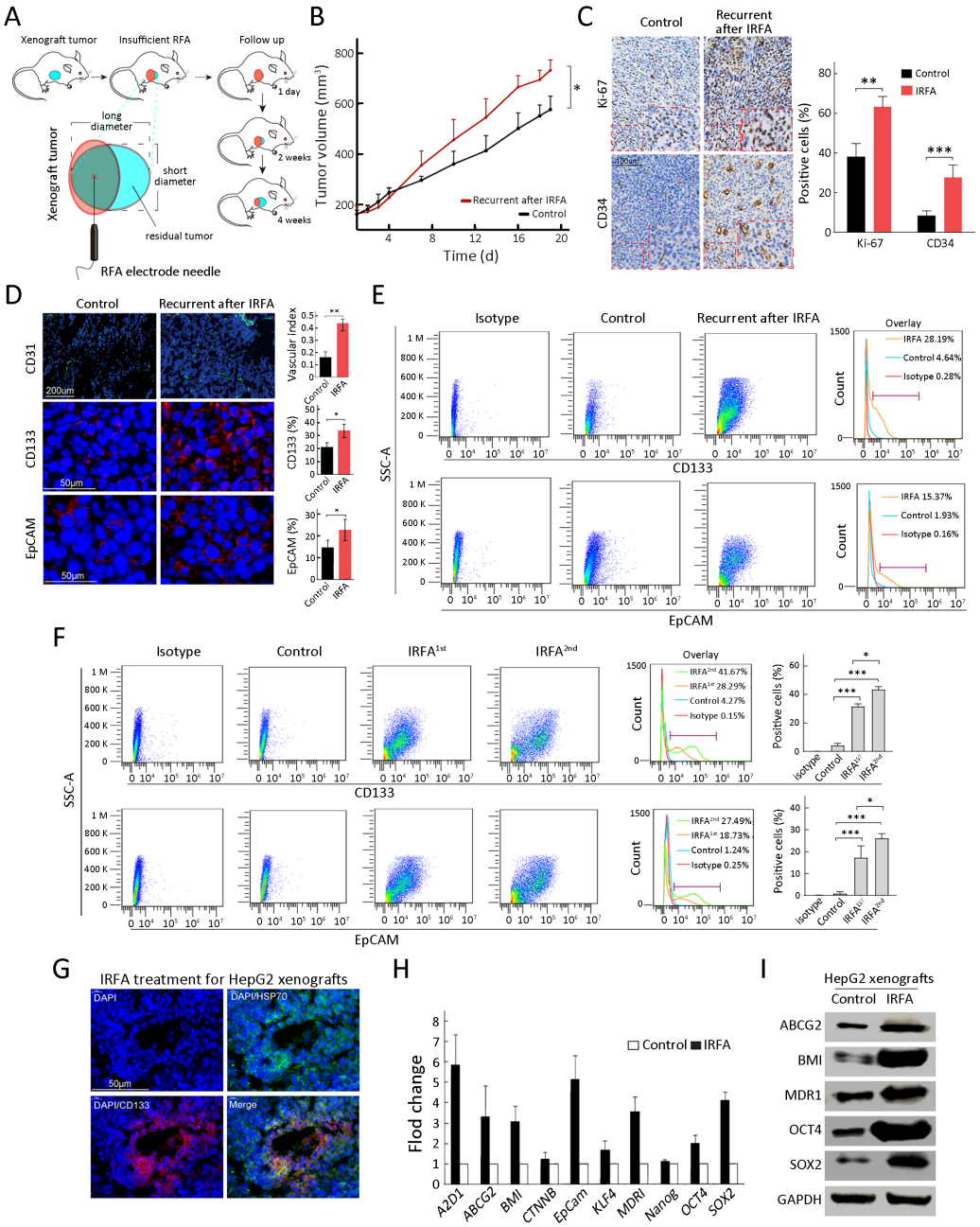

Figure 3 Enrichment of TICs after IRFA treatment *in vivo*. (A) A schematic diagram for IRFA treatment in mice xenografts. Orange area: IRFA zone; (B) Tumor growth of HepG2 xenografts in NOD/SCID mice treated with/without IRFA (n=6/group) (P<0.05); (C) Expressions of Ki-67 and CD34 in xenograft tumors were detected by immunohistochemistry assay; (D) Vascular index and percentage of CD133⁺, CD31⁺ and EpCAM⁺ in HepG2 xenografts in NOD/SCID mice were detected by immunofluorescence staining. Nuclei were stained with DAPI (blue); (E,F) CD133⁺ and EpCAM⁺ subpopulation of HepG2 xenografts were analyzed by FCA; (G) HSP70⁺ and CD133⁺ cells at the fringe of post-RFA necrosis lesions after 48 h treatment; (H,I) Expression levels of stem cell-related genes in xenografts are analyzed by qRT-PCR (H) and Western blot (I). Bar graphs (in C,D,F,H) are presented as $\bar{x}\pm s$. TIC, tumor-initiating cell; IRFA, insufficient radiofrequency ablation; RFA, radiofrequency ablation; EpCAM, epithelial cell adhesion molecule; FCA, flow cytometric analysis; SSC-A, side scatter area; HSP, heat shock protein; qRT-PCR, quantitative real-time polymerase chain reaction. *, P<0.05; **, P<0.01; ***, P<0.001.

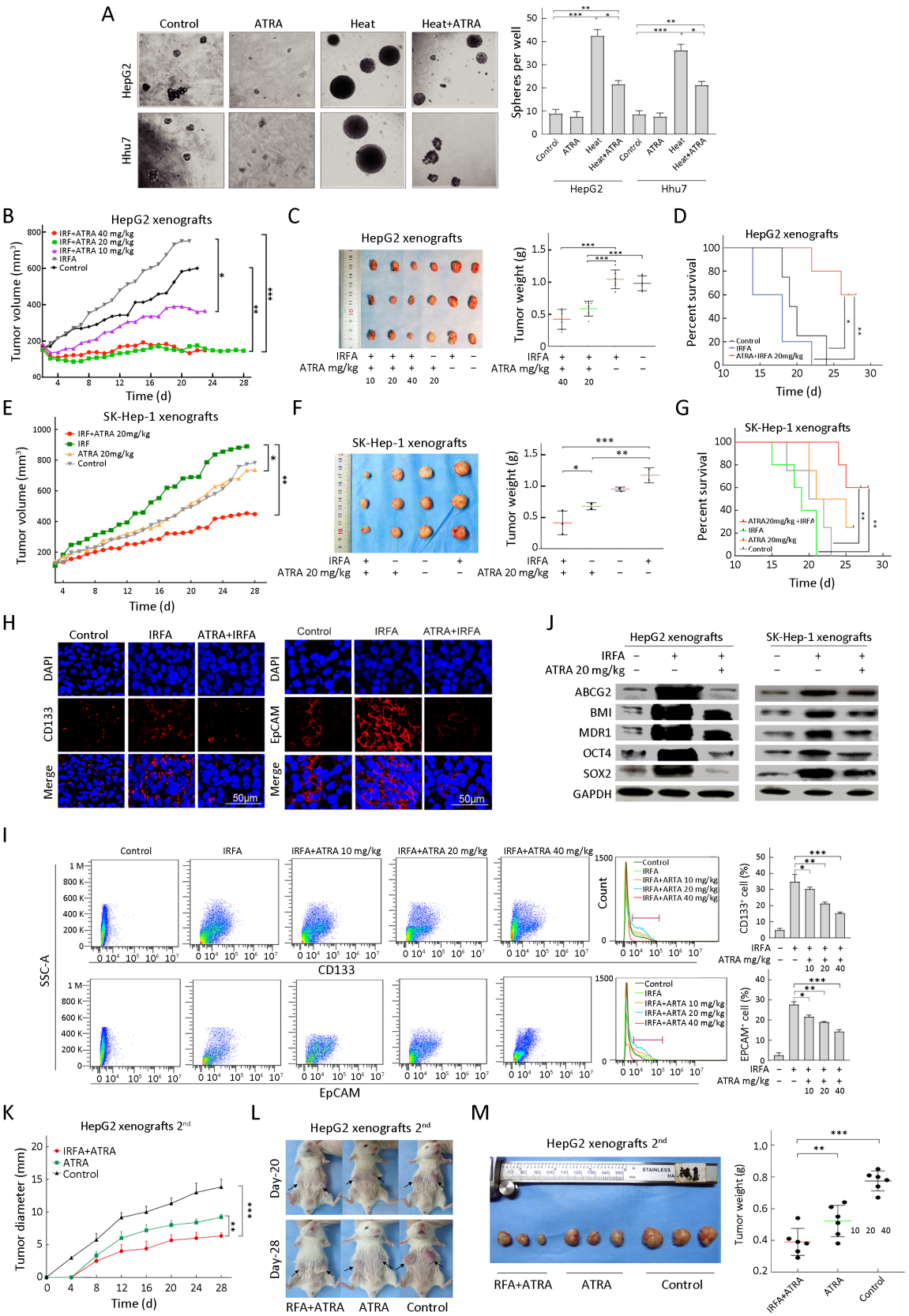

Figure 4 ATRA combination therapy suppresses growth of recurrent HCC after IRFA by inhibition of TICs. (A) Representative phase contrast micrographs of the spheroid forming efficiency of HepG2 cells treated with or without heat and ATRA; (B) Tumor growth of different administered groups of HepG2 xenografts in NOD/SCID mice (n=3/group). Tumor size was measured with a caliper rule every 2 days; (C) Photographs show tumors and tumor weight for each group of HepG2 xenografts; (D) Kaplan-Meier survival curves of NOD/SCID mice after the treatments showed the combination therapy of RFA and ATRA (red line) had the best survival outcome; (E–G) Combination therapy of 20 mg/kg ATRA indicated slowest tumor growth (E), smallest tumor weight (F) and longest survival time (G) in the SK-Hep-1 xenografts (n=3/group); (H) Immunofluorescence staining of $CD133^+$ and $EpCAM^+$ cells in HepG2 xenograft. Positive cells were stained as red signal; nuclei were stained with DAPI (blue); (I) Proportions of $CD133^+$ and $EpCAM^+$ subpopulation of HepG2 xenografts with different treatment were analyzed by FCA; (J) Expression of the stem cell-related genes was inhibited in the combination treatment tumors compared with the RFA alone by Western blot analysis; (K–M) Tumor diameter (measured with a caliper rule every 2 days), photographs and tumor weight of the second HepG2 xenografts treated with 20 mg/kg ATRA or combination therapy. Data in (A, I) are presented as $\bar{x}\pm s$. ATRA, all-trans retinoic acid; HCC, hepatocellular carcinoma; IRFA, insufficient radiofrequency ablation; TIC, tumor-initiating cell; RFA, radiofrequency ablation; EpCAM, epithelial cell adhesion molecule; DAPI, 4',6-diamidino-2-phenylindole; FCA, flow cytometric analysis. *, P<0.05; **, P<0.01; ***, P<0.001.

$EpCAM^+$ cells were greatly decreased in the 40 mg/kg ATRA combination treatment group compared with the IRFA alone group (*Figure 4I*, CD133: 17.8%±1.5% *vs.* 35.6%±4.7%, P<0.001; EpCAM: 15.1%±2.1% *vs.* 38.0%±2.8% , P<0.001). Meanwhile, the expression of other stem cell related genes, including *BMI*, *OCT4*, *SOX2*, *ABCG2* and *MDR1*, was also attenuated in the ATRA combination group compared to the IRFA group (*Figure 4J*).

To further confirm the inhibitory effect of ATRA on TICs, serial passages were performed. After the second tumorigenicity assay, the tumor formation rate was effectively suppressed in the ATRA+IRFA group compared with that in the control group (P<0.05) (*Table 2*). Moreover, the combination group displayed the slowest tumor growth (6.3±0.5 mm *vs.* 9.2±0.5 mm for the ATRA group, P<0.01; 6.3±0.5 mm *vs.* 13.8±1.2 mm for the control group, P<0.001) (*Figure 4K*), the smallest tumor size (*Figure 4L*) and the lightest tumor weight (*Figure 4M*) among the three groups. During 4 weeks of follow-up, there were no significant differences in the body weights of the mice among the three groups after treatment (*Supplementary Figure S1A*), and no visible histopathological damage in the tissues of essential organs, including the heart, liver, spleen, lung and kidney, was observed by H&E staining (*Supplementary Figure S1B*).

Taken together, these results suggested that ATRA could effectively improve the therapeutic efficiency of IRFA by decreasing the TICs in liver cancer. Moreover, no significant apparent adverse effects were observed in mice treated with ATRA.

ATRA triggers apoptosis and suppresses TICs by inhibiting PI3K/AKT pathway

Consistent with the previous study, ATRA treatment suppressed the proliferation ability of post-IRFA recurrent tumors, as measured by the percentage of $Ki\text{-}67^+$ cells (*Figure 5A*) but enhanced the tumor cell apoptosis, as detected by TUNEL analysis (*Figure 5B*). Previously, it was reported that IRFA promoted the growth through PI3K/Akt/HIF-1α signaling (23). Consistently, the expression of *p-PI3K*, *p-AKT* and *p-mTOR* was upregulated by IRFA, but the increase in these genes was further downregulated by ATRA treatment in HepG2 xenografts (*Figure 5C*). Furthermore, higher expression levels of

Table 2 Effect of adjuvant ATRA on HepG2 tumor formatting rate after second transplantation

Variables	Amount of tumor [n/N* (%)]			P** for ATRA+IRFA	
	Control	ATRA	IRFA+ATRA	*vs.* Control	*vs.* ATRA
Day 3	4/12 (33.3)	0/12 (0)	0/12 (0)	0.047	–
Day 7	7/12 (58.3)	2/12 (16.7)	1/12 (8.3)	0.027	1
Day 12	10/12 (83.3)	4/12 (33.3)	3/12 (25.0)	0.012	1
Diameter at end-point ($\bar{x}\pm s$) (mm)	13.8±1.2	9.2±0.5	6.3±0.5	0.007	0.032

ATRA, all-trans retinoic acid; IRFA, insufficient radiofrequency ablation. *, n: the actual number of tumors formed; N: the number of transplanted tumors. **, Fisher's exact test was used to analyze the difference in tumor formatting rate after the second tumor formation rate between different groups.

p-PI3K, *p-AKT* and *p-mTOR* were also detected in HepG2 cells subjected to heat intervention, while the increase in these genes was further attenuated by either ARTA treatment or an AKT inhibitor (*Figure 5D*). These results demonstrated that IRFA might promote recurrent tumor growth by enrichment of TICs through the PI3K/AKT pathway, while ATRA or an AKT inhibitor could block the promotion effect of IRFA by eliminating the increase of PI3K/AKT pathway. Thus, the combination of ATRA or AKT inhibitors might be a potential agent to increase the therapeutic efficiency of RFA.

Discussion

RFA is a safe and effective treatment for early-stage HCC. However, local recurrence is common and progresses rapidly (24). Therefore, it is important to investigate the biological behavior and underlying mechanisms of recurrent HCC after RFA to improve the prognosis of HCC patients. It has been reported previously that IRFA promotes HCC progression by enrichment of TICs (22). Here, we not only conformed the enrichment of TICs after IRFA, which was responsible for tumor progression after treatment but also delivered a combination treatment with ATRA to improve the efficiency of RFA by eliminating TICs in HCC.

First, we collected a cohort of 120 cases patients with HCC who received ultrasound guided percutaneous RFA treatment. Eleven of 120 (9.2%) patients were diagnosed with local recurrence by CECT/MRI after RFA treatment, which was consistent with the previously reported recurrent rate of approximately 8%–15% (5). Additionally, we found that the tumor stem cell markers (CD133 and EpCAM) were highly expressed in recurrent HCCs compared with initial HCCs. These results provide a reference for clinical practice. The biological behavior of

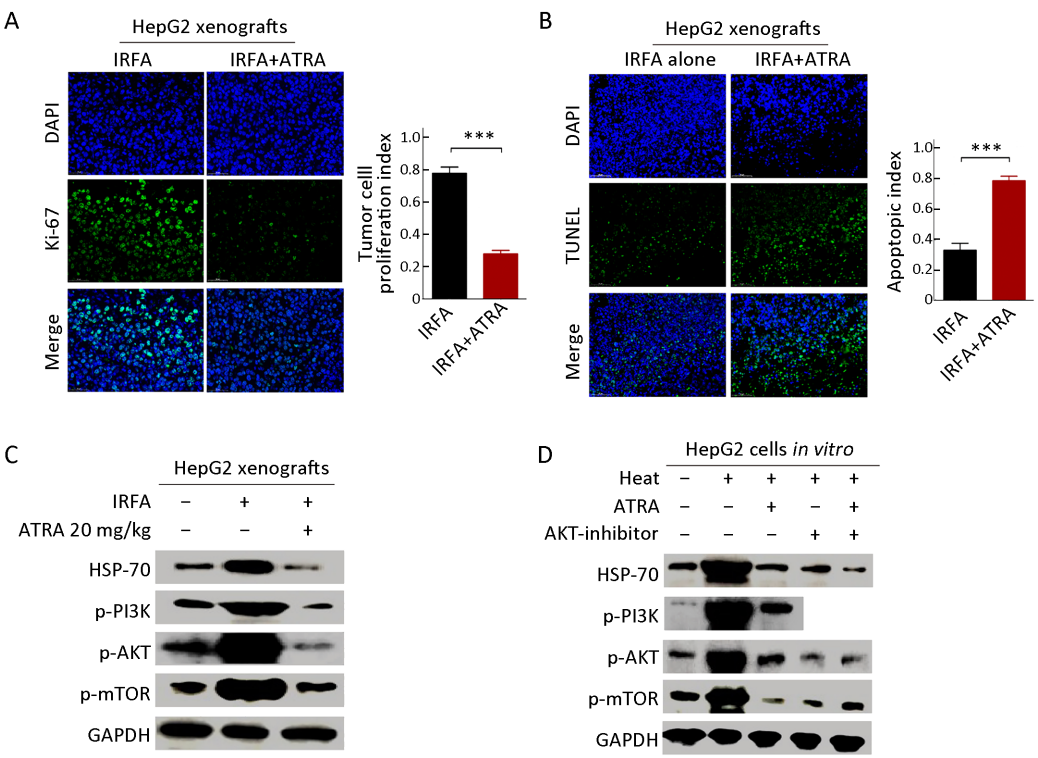

Figure 5 ATRA suppresses growth and triggers apoptosis by inhibiting PI3K/AKT pathway. (A,B) Immunofluorescence staining was performed to analyze the expression of Ki-67 (A) and TUNEL (B) in HepG2 xenografts treated with combination therapy or IRFA alone. Positive cells were stained with green signal, nuclei were stained with DAPI (blue). The bar graph depicts quantification of Ki-67$^+$ and TUNEL$^+$ cells (right panels). Data are presented as $\bar{x}\pm s$; (C,D) Western blot was performed to detect PI3K/AKT signaling pathway. PI3K/AKT pathway, which was activated by IRFA treatment, could be downregulated by combinatorial therapy, compared to the control group. IRFA, insufficient radiofrequency ablation; ATRA, all-trans retinoic acid; RFA, radiofrequency ablation; DAPI, 4',6-diamidino-2-phenylindole. ***, P<0.001.

recurrent HCCs is more aggressive than that of primary HCCs. Moreover, during a follow-up period of 160 months in this study, we found that the overall survival time of recurrent HCC patients was significant poorer than those without recurrence. This result was also consistent with previous reports (25). Thus, combination treatment with other adjuvant agents is required to further improve the outcome.

Furthermore, the malignant potential of heat-treated HCC cells was determined *in vitro*. Since HSP70 expression was closely associated with the malignant phenotype of post-RFA treatment, such as tumor cell proliferation and distant metastasis (26,27), the optimal heat-treatment conditions including temperature and time, were determined according to the HSP70 expression in this study and a previous one (20). In this study, the cells were treated with the maximum of HSP70 protein at 42 °C for 6 h. In a previous report by Yoshida *et al.*, heat treatment at 45 °C and 50 °C for 10 min promoted EMT and enhanced the malignant potential of HCC (28). Calderwood *et al.* revealed that the HSPs are expressed in particular quantities after heat shock, and these proteins are regarded as the protective reactions of tumor cells. High HSP expression could promote tumor cell proliferation, and it could play a key role in the TIC renewal (29). Consistently, in our study, heat intervention enhanced the sphere-forming ability of HCC cells, the TIC proportions of $CD133^+$ and $EpCAM^+$ subpopulations and the stem cell-related gene expression, including *ABCG2*, *BMI*, *MDR1*, *OCT4* and *SOX2*. In addition, malignant potential post-IRFA therapy was determined *in vivo* in NOD/SCID mouse xenografts. The residual tumor cells after IRFA therapy indicated a quick relapse and rapid growth. Meanwhile, the enrichment of TICs was also verified in recurrent xenografts compared with control xenografts (30). Taken together, these *in vitro* and *in vivo* data suggested that either heat or RFA treatment promoted the proliferative and invasive potential of HCC by enriching TICs.

It is known that inducing the TIC differentiation is an appealing therapeutic strategy for cancer. ATRA, as one of the strongest inducers of differentiation, exerts anticancer effects by inducing apoptosis and differentiation of cancer cells as well as TICs. Here, we evaluated the effects of ATAR combination therapy on HCC TIC differentiation in recurrent tumors after IRFA treatment and developed a novel chemotherapeutic approach. Consistent with a previous study (18), we found that ATRA, as a single anticancer chemotherapeutic drug, showed a slight suppressive effect on tumor growth. More importantly, ATRA could significantly inhibit the tumor proliferation and growth of relapsed cancer after IRFA therapy *in vivo*. This antitumor effect might contribute to ATRA-induced differentiation of HCC TICs. Previously, Zhang *et al.* found that ATRA could induce the differentiation of $EpCAM^+$ HCC TICs and enhance the effect of cisplatin (19). In this study, we found that the inhibition of ARTA on both $CD133^+$ and $EpCAM^+$ HCC TICs subsequently decreased the relapse of RFA treatment. At the molecular level, the potential aggressive ability of cancer cells could be facilitated via activating PI3K/AKT pathway (31). We further found that IRFA might promote recurrent tumor growth by enrichment of TICs through the PI3K/AKT pathway, while ATRA or AKT inhibitors could block the promotion effect of IRFA by eliminating the increase of PI3K/AKT pathway. Thus, the combination of ATRA or AKT inhibitors might be a potential strategy to increase the therapeutic efficiency of RFA. However, clinical research is still required to evaluate the efficacy and safety of the combination of ARTA with RFA treatment in HCC.

Conclusions

Our data revealed that there is an enrichment effect of TICs after RFA therapy and that targeting TICs might be an effective strategy to improve the RFA therapeutic efficacy of solid cancers. Hence, ARTA, a known TIC differentiation inducer, presents an alternative opportunity for the development of better therapeutic strategies used in combination with RFA.

Acknowledgements

This study was supported by National Natural Science Foundation of China (No. 81773286, 81971718, and 81772632); Beijing Baiqianwan Talents Project (No. 2020A47) and Science Foundation of Peiking University Cancer Hospital (No. 2020-9).

Footnote

Conflicts of Interest: The authors have no conflicts of interest to declare.

References

1. Sung H, Ferlay J, Siegel RL, et al. Global cancer statistics 2020: GLOBOCAN estimates of incidence

and mortality worldwide for 36 cancers in 185 countries. CA Cancer J Clin 2021;71:209-49.
2. Feng RM, Zong YN, Cao SM, et al. Current cancer situation in China: good or bad news from the 2018 Global Cancer Statistics? Cancer Commun (Lond) 2019;39:22.
3. Shiina S, Sato K, Tateishi R, et al. Percutaneous ablation for hepatocellular carcinoma: Comparison of various ablation techniques and surgery. Can J Gastroenterol Hepatol 2018;2018:4756147.
4. Ma X, Ouyang H, Wang S, et al. Histogram analysis of apparent diffusion coefficient predicts response to radiofrequency ablation in hepatocellular carcinoma. Chin J Cancer Res 2019;31:366-74.
5. Yoon JS, Lee YR, Kweon YO, et al. Comparison of acoustic radiation force impulse elastography and transient elastography for prediction of hepatocellular carcinoma recurrence after radiofrequency ablation. Eur J Gastroenterol Hepatol 2018;30:1230-6.
6. Taniguchi S, Elhance A, Van Duzer A, et al. Tumor-initiating cells establish an IL-33-TGF-β niche signaling loop to promote cancer progression. Science 2020;369:eaay1813.
7. Liu YC, Yeh CT, Lin KH. Cancer stem cell functions in hepatocellular carcinoma and comprehensive therapeutic strategies. Cells 2020;9:1331.
8. Wu Y, Zhang J, Zhang X, et al. Cancer stem cells: A potential breakthrough in HCC-targeted therapy. Front Pharmacol 2020;11:198.
9. Ouyang Y, Liu K, Hao M, et al. Radiofrequency ablation-increased CXCL10 is associated with earlier recurrence of hepatocellular carcinoma by promoting stemness. Tumour Biol 2016;37:3697-704.
10. Liu K, Hao M, Ouyang Y, et al. CD133$^+$ cancer stem cells promoted by VEGF accelerate the recurrence of hepatocellular carcinoma. Sci Rep 2017;7:41499.
11. Tan L, Chen S, Wei G, et al. Sublethal heat treatment of hepatocellular carcinoma promotes intrahepatic metastasis and stemness in a VEGFR1-dependent manner. Cancer Lett 2019;460:29-40.
12. Nguyen CH, Grandits AM, Vassiliou GS, et al. Evi1 counteracts anti-leukemic and stem cell inhibitory effects of all-trans retinoic acid on Flt3-ITD/Npm1c-driven acute myeloid leukemia cells. Biomedicines 2020;8:385.
13. Bouriez D, Giraud J, Gronnier C, et al. Efficiency of all-trans retinoic acid on gastric cancer: A narrative literature review. Int J Mol Sci 2018;19:3388.
14. Ju J, Wang N, Wang X, et al. A novel all-trans retinoic acid derivative inhibits proliferation and induces differentiation of human gastric carcinoma xenografts via up-regulating retinoic acid receptor beta. Am J Transl Res 2015;7:856-65.
15. Brugnoli F, Grassilli S, Cardinale V, et al. Vav1 sustains the *in vitro* differentiation of normal and tumor precursors to insulin producing cells induced by all-trans retinoic acid (ATRA). Stem Cell Rev Rep 2021;17:673-84.
16. Herreros-Villanueva M, Er TK, Bujanda L. Retinoic acid reduces stem cell-like features in pancreatic cancer cells. Pancreas 2015;44:918-24.
17. Zheng Z, Liu J, Yang Z, et al. MicroRNA-452 promotes stem-like cells of hepatocellular carcinoma by inhibiting Sox7 involving Wnt/beta-catenin signaling pathway. Oncotarget 2016;7:28000-12.
18. Cui J, Gong M, He Y, et al. All-trans retinoic acid inhibits proliferation, migration, invasion and induces differentiation of hepa1-6 cells through reversing EMT *in vitro*. Int J Oncol 2016;48:349-57.
19. Zhang Y, Guan DX, Shi J, et al. All-trans retinoic acid potentiates the chemotherapeutic effect of cisplatin by inducing differentiation of tumor initiating cells in liver cancer. J Hepatol 2013;59:1255-63.
20. Yang W, Cui M, Lee J, et al. Heat shock protein inhibitor, quercetin, as a novel adjuvant agent to improve radiofrequency ablation-induced tumor destruction and its molecular mechanism. Chin J Cancer Res 2016;28:19-28.
21. Guo T, Wen XZ, Li ZY, et al. ISL1 predicts poor outcomes for patients with gastric cancer and drives tumor progression through binding to the ZEB1 promoter together with SETD7. Cell Death Dis 2019;10:33.
22. Yuan CW, Wang ZC, Liu K, et al. Incomplete radiofrequency ablation promotes the development of CD133$^+$ cancer stem cells in hepatocellular carcinoma cell line HepG2 via inducing SOX9 expression. Hepatobiliary Pancreat Dis Int 2018;17:416-22.
23. Wan J, Wu W, Chen Y, et al. Insufficient radiofrequency ablation promotes the growth of non-small cell lung cancer cells through PI3K/Akt/HIF-1alpha signals. Acta Biochim Biophys Sin (Shanghai)

2016;48:371-7.
24. Zhang N, Li H, Qin C, et al. Insufficient radiofrequency ablation promotes the metastasis of residual hepatocellular carcinoma cells via upregulating flotillin proteins. J Cancer Res Clin Oncol 2019;145:895-907.
25. Xie X, Jiang C, Peng Z, et al. Local recurrence after radiofrequency ablation of hepatocellular carcinoma: Treatment choice and outcome. J Gastrointest Surg 2015;19:1466-75.
26. Song HB. Possible involvement of HSP70 in pancreatic cancer cell proliferation after heat exposure and impact on RFA postoperative patient prognosis. Biochem Biophys Rep 2019;20:100700.
27. Ahmed M, Kumar G, Gourevitch S, et al. Radiofrequency ablation (RFA)-induced systemic tumor growth can be reduced by suppression of resultant heat shock proteins. Int J Hyperthermia 2018;34:934-42.
28. Yoshida S, Kornek M, Ikenaga N, et al. Sublethal heat treatment promotes epithelial-mesenchymal transition and enhances the malignant potential of hepatocellular carcinoma. Hepatology 2013;58: 1667-80.
29. Calderwood SK, Gong J. Heat shock proteins promote cancer: It's a protection racket. Trends Biochem Sci 2016;41:311-23.
30. Diorio C, Robinson PD, Ammann RA, et al. Guideline for the management of clostridium difficile infection in children and adolescents with cancer and pediatric hematopoietic stem-cell transplantation recipients. J Clin Oncol 2018;36:3162-71.
31. Deng X, Ao S, Hou J, et al. Prognostic significance of periostin in colorectal cancer. Chin J Cancer Res 2019;31:547-56.

Cite this article as: Wang S, Liu J, Wu H, Jiang A, Zhao K, Yan K, Wu W, Han H, Zhang Y, Yang W. All-trans retinoic acid (ATRA) inhibits insufficient radiofrequency ablation (IRFA)-induced enrichment of tumor-initiating cells in hepatocellular carcinoma. Chin J Cancer Res 2021;33(6):694-707. doi: 10.21147/j.issn.1000-9604.2021.06.06

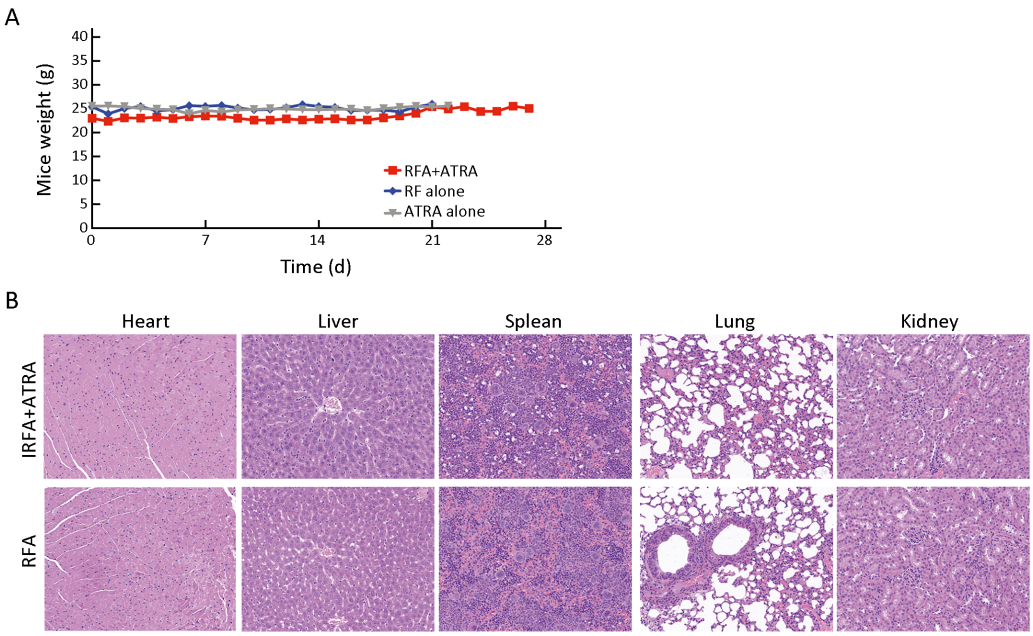

Figure S1 No obvious toxicity of ATRA on mice bearing HepG2 tumors. (A) Mice weight in different treatment groups was measured every 2 days during experiment; (B) H&E staining for tissues of heart, liver, spleen, lung and kidney demonstrated no obvious histopathological damage to the important organs in the indicated groups (200×). RFA, radiofrequency ablation; ATRA, all-trans retinoic acid; IRFA, insufficient radiofrequency ablation; H&E, hematoxylin & eosin.